Available online at www.sciencedirect.com
ScienceDirect
Agricultural and Forest Meteorology 145 (2007) 195–205
AGRICULTURAL AND FOREST METEOROLOGY
www.elsevier.com/locate/agrformet

Measured winds about a thick hedge

Andrée Tuzet [a], John D. Wilson [b,*]

[a] *Institut National de la Recherche Agronomique (INRA), Paris, France*
[b] *Department of Earth & Atmospheric Sciences, University of Alberta, Edmonton, Canada*

Received 4 June 2006; received in revised form 10 March 2007; accepted 25 April 2007

Abstract

We measured mean windspeed and turbulent kinetic energy (15 min averaging intervals) in the region of a tall cypress hedge (height $H = 8$ m; thickness $X = 3$ m), the observed patterns resembling those previously reported for dense, natural shelterbelts, except in circumstances where secondary shelterbelts at the site played a role. Along a transect at height $z = H/4$, minimum mean windspeed always occurred at the anemometer closest to the hedge ($H/4$ from the downwind edge), and mean windspeed at that point was only about 20–25% of the upwind value, with weak sensitivity to thermal stratification and to the orientation of the approaching wind. We also examined time series of velocity from sonic anemometers placed against the upstream and downstream faces of the hedge, forming statistics over averaging intervals selected by the criterion that lowpass filtered wind direction should never reverse to exchange the 'upwind' and 'downwind' sides. Whatever the far upwind angle of approach and corresponding angle of incidence on the upwind face, the mean wind emerged from the downwind face aligned with the normal.

Keywords: Averaging; Drag; Hedge; Shelter; Turbulence; Wind; Windbreak

1. Introduction

There have been relatively few field studies of the wind shelter provided by a pruned 'hedge', i.e. a row (or rows) of trees forming a visually impermeable barrier whose height (H) and thickness (X) are unnaturally regular. Perhaps this is because in modern agriculture the value of a hedge has tended to lie, not so much in its pleasing appearance, but in its function, so that for decades farmers have been advised that a somewhat permeable windbreak is optimally effective against the wind. Even so the dense, pruned hedge remains a common sight in many countries, and it is pertinent to stress the many (potentially) co-existent functions it may have: as a means to beautify the environment, as a provider of privacy, as a barrier against the wind or sun, as a habitat for birds, insects and animals, and/or as a barrier to stock movement. Agate (2002) writes ''In the recent past, hedges were seen by many farmers, especially most arable farmers, only in economic terms. From this viewpoint they were seen as expensive to maintain, wasting valuable land, preventing efficient use of large machines, and harbouring pests. Possibly this view is now changing. Well maintained hedges are coming to be seen as an asset for the farmer, to be managed well for the benefit of the farm business, as well as for their wildlife, stock, amenity, and landscape values. However, hedges are continuing be lost at a high rate, because on many farms the economic argument has to win''.

Here we report measurements[1] quantifying the wind environment around a dense cypress hedge, standing in

* Corresponding author. Tel.: +1 780 492 0353.
E-mail address: jaydee.uu@ualberta.ca (J.D. Wilson).

[1] These measurements were part of a more comprehensive study, whose perspective covered microclimatology, hydrology, crop physiology and bio-diversity.

0168-1923/$ – see front matter © 2007 Elsevier B.V. All rights reserved.
doi:10.1016/j.agrformet.2007.04.013

a complex farm setting. In Section 2 we describe the site and instrumentation, then in Section 3 we deduce as best we can the broad pattern of the wind and turbulence around the hedge. For readers familiar already with shelter from a dense windbreak the main novelty will be found to lie in Section 3.4, concerning velocity statistics at the entry and exit faces as seen by sonic anemometers, and in Section 3.5 where by integrating the momentum equation across the hedge we suggest a means to estimate a drag parameter.

2. The experiment

The experiment took place 20–28 August 2001 on a private farm at Villepreux (near Paris, France). Fig. 1, reconstructed from a Google image and GPS surveying, shows the site was complex, due to its gentle topography, and more particularly due to intersecting belts of pruned hedges (features A and C) and lines of trees (B, D and E). The principal windbreak (A) was a dense Leyland Cypress hedge (*Cupressus leylandii*, see photograph, Fig. 2) of height $H = 8$ m and thickness $X = 3$ m (at its northern end a belt of trees, B, increased its width). Its optical porosity was zero, however as emphasized by Zhou et al. (2004) "optical porosity as a 2D structural descriptor is unable to sufficiently represent the aerodynamic structure of a tree shelterbelt". The foliage surface area density was estimated[2] (Caroupanapoullé, 2004) to be of order 1 $m^2\ m^{-3}$ in the shaded interior of the hedge, while in the sunlit outer 15 cm it was close to 15 $m^2\ m^{-3}$. East of the main hedge (A) the surface was in short stubble (height about 20 cm); on the west side lay a bare ploughed field, sloping down towards a line of trees (E). Another thick hedge (C) ran roughly east–west to north of the measurement site, while a line of weeping willows (D, *Salix babylonica*, height about 20 m) ran beside a drainage ditch on the southern boundary. Also shown in Fig. 1 are other groves or irregular lines of trees: in short, *nowhere* on this site could one be assured that the structure of the wind was in equilibrium with the surface, and so describable under the rubric of Monin-Obukhov similarity theory (MOST).

We placed anemometers so as to be able to summarize the effects on the wind of the "main" shelterbelt (A). Fig. 1 indicates a (discontinuous) transect, at each extremity of which stood a tall mast, and along which cup anemometers (CIMEL CE155) were placed at height $z = 2$ m. Positions of the cups, measured along the normal

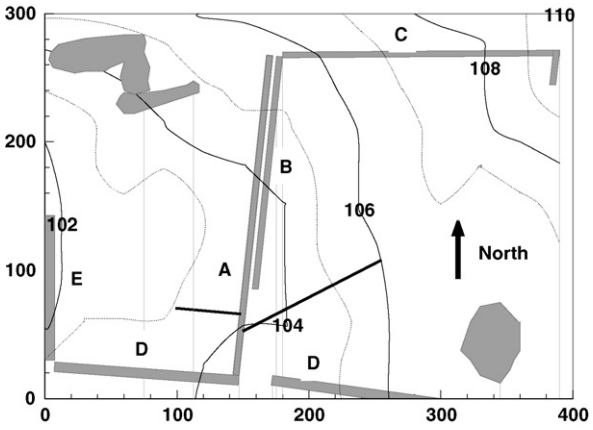

Fig. 1. Scale drawing of the site (horizontal distances in metres; elevation contours in metres above sea-level, with 1 m interval). The principal windbreak (A) was a cypress hedge (see photograph, Fig. 2). Cup anemometers were placed at $z = 2$ m along the indicated transect (dark narrow line, discontinuous at hedge), at positions specified in the text; the time series measurements of Section 3.4 stem from sonics placed approximately at the intersection of the cup transect with the main hedge. At each extremity of the transect, tall masts were instrumented with cup anemometers, and the eastern mast carried the 'reference' sonic anemometer, at $z = 5$ m.

to the shelterbelt and from an origin at its centre, were (west side) $|x/H| = (6.25, 5, 3.75, 2, 1, 0.5)$ and (east side) $|x/H| = (0.43, 0.85, 1.7, 4.25, 8.5, 12.75)$; alternatively in dimensional terms (west side) $|x| = (50, 40, 30, 16, 8, 4)$ m and (east side) $|x| = (3.4, 6.8, 13.6, 34, 68, 102)$ m. These west and east anemometer transects intersected the main hedge at distances of respectively (45 and 35 m) or ($5.6H$ and $4.4H$) from the bounding southern line of

Fig. 2. Eastern side of the cypress hedge "A" (height $H = 8$ m, thickness $X = 3$ m) looking (roughly) south towards the access break in the willows ("D", not visible). A CSAT3 and a Gill sonic anemometer are visible, placed against the face of the hedge.

[2] By optimizing the fit of a radiation model to measurements of beam and diffuse solar radiation.

willows (D), a distance smaller than one would usually wish in the context of 'end effects'. However the notion of placing instruments at some minimum acceptable distance from ends of a windbreak to avoid end effects belongs with and stems from a concept that does not apply here, namely the concept of the flow being statistically invariant along the direction parallel to the hedge (A): patently that is not a reasonable expectation at this site, the willows (D) constituting only one of several factors destroying the symmetry.

In addition to the cup anemometers, five three-dimensional sonic anemometers[3] were available. One Gill sonic, at $z = 5$ m on the east tower at $|x| = 102$ m, served as the reference whence we derived values of the friction velocity u_{*0} and Obukhov length L; the other four sonics were arranged (consecutively) in three configurations: along the transect at $z = 2$ m; hard against or above the hedge; or on a profile 16 m due west from the hedge.

The orientation of the main hedge A was sufficiently close to north–south that we shall name it so, and thereby define a convenient angular origin (i.e. our 0–180° axis). A local mean wind direction in that frame will be denoted θ, so $\theta = 0°, 90°, 180°$ and 270°, respectively denote mean winds *from* the (nominal) north (more strictly, parallel to the hedge), east, south and west. The notation θ_0 will indicate the *undisturbed* mean wind direction, i.e. as determined at a point outside the wakes of all windbreaks (for example on the east tower during winds from the sector northeast through east-southeast), and for convenience we shall define ϕ_0 as the deviation of the orientation θ_0 away from the *normal* to the upwind face of the hedge (with similar definitions for ϕ_1, ϕ_2, the deviations from the normal of the mean wind direction measured on the upwind and downwind faces). We denote by x/H the distance down the normal to the windbreak, measured from the centre-point of the hedge; by (u, v) the wind components respectively normal (east–west) and parallel (north–south) to the windbreak, with $u > 0$ designating a wind that approaches the hedge from the east side and $v > 0$ designating a component from the 'north'; and by (U, V) the average winds, with $u' = u - U, v' = v - V$ the fluctuations.

3. Results

Fig. 3 gives several profiles of the mean cup windspeed on the eastern (reference) tower

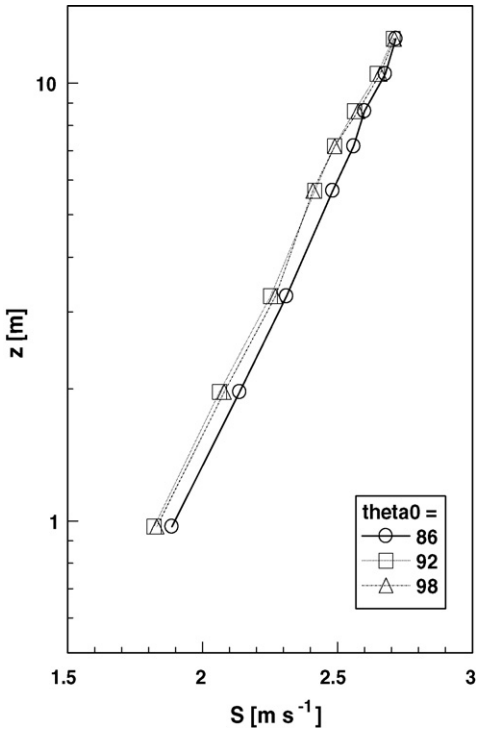

Fig. 3. Profiles of 30 min mean cup windspeed $S_0(z)$, for nearly easterly ($\theta_0 \sim 90°$) approach flows.

($x = 102$ m), during easterly winds. In addition to giving an indication of the quality of the cup anemometers, these profiles confirm the hoped-for existence of a semi-logarithmic profile at the east reference tower in easterly winds, and permit to deduce the surface roughness length: from five periods with $|L| > 15$ m and basing the estimate on anemometers below $z = 3.25$ m ($z/|L| < 0.21$), we computed that $0.2 \leq z_{0E} \leq 0.5$ cm with a mean value of $z_{0E} = 0.4$ cm. This is surprisingly small, but we have no reason to doubt the equipment or the calculation. There is no choice but to conclude that one may not interpret these profiles as necessarily being in equilibrium with the surface.

3.1. Transects of mean windspeed with strong normal component

We begin with the transect of normalized mean windspeed S/S_0 (or 'relative windspeed') across the main windbreak during winds with a strong component normal to the windbreak (all contributing 15 min runs had $S_0 \geq 1.5$ m s^{-1}). The solid points in Fig. 4 are transects during winds that were oriented normal to the windbreak (for consistency we display transects such that negative x/H always denotes the *upwind* side),

[3] Two Campbell Scientific Inc. (CSI) model CSAT3 sampled at 5 Hz on a CSI CR10X datalogger; two Gill R2's sampled at 20.8 Hz on a CSI CR21X, and one Gill sampled using the data-acquisition program 'Edisol' on a laptop.

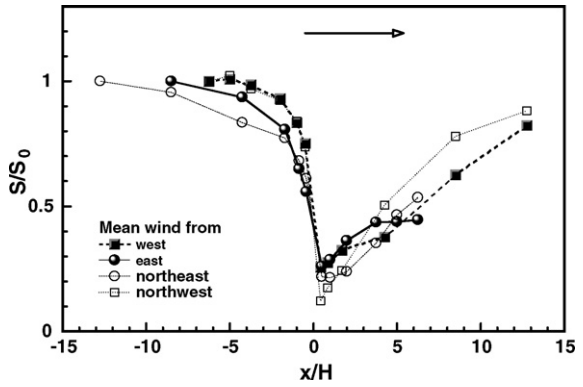

Fig. 4. Transects along $z = 2$ m of relative cup windspeed S/S_0, for nearly perpendicular approach flows (of speed S_0) from east and west, as well as for 45° oblique flows. Each transect is an average over several 15 min records (see text for details). Convention of the diagrams is that positive x is always the downwind side of the hedge.

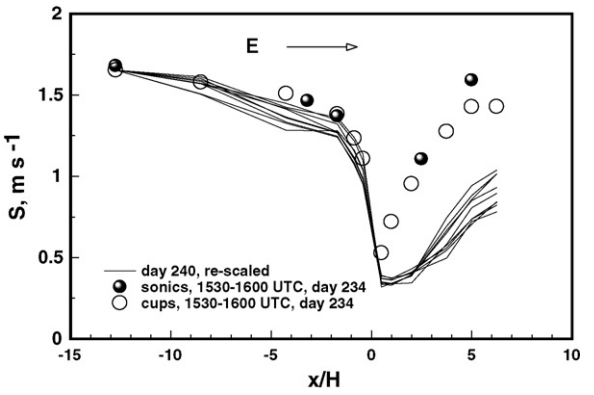

Fig. 5. Transects of cup windspeed S for flows from the NE. Observations from the cups and sonics during a single thermally unstable period ($L = -6$ m, $\theta_0 = 57°$, $\sigma_{\theta_0} = 41°$) are compared with nine re-scaled wind reduction curves from a much windier, overcast day (see text for details). Positive x is the upwind side of the hedge. The easternmost sonic stood at $z = 5$ m whereas all other instruments stood at $z = 2$ m, thus the speed it indicated has been reduced by the factor $\ln(2/z_{0E})/\ln(5/z_{0E}) = 0.87$.

showing the mean of five runs for each of which mean wind direction $\theta_0 = 90 \pm 3°$ (east wind), and the mean of four runs for each of which $\theta_0 = 270 \pm 3°$ (west wind). In these normal winds ($\phi_0 = 0 \pm 3°$) the main shelterbelt reduced the mean windspeed to (a minimum of) only 25% of its upwind strength S_0, with the minimum speed occurring at the closest leeward point, i.e. in the immediate lee of the hedge (rather than at $x/H \sim 3$–5, as occurs for thin, artificial windbreaks). The observed location and depth of the relative windspeed curve at the point of minimum windspeed are consistent with what had earlier been reported for dense, natural shelterbelts, both on the basis of observations (Rider, 1952, Table 1; van Eimern et al., 1964, e.g. Fig. 4; Plate, 1971, Fig. 6; Takahashi, 1978; Heisler and DeWalle, 1988, Fig. 2) and computations (Wang and Takle, 1996, Fig. 4a). Also shown in Fig. 4 are mean transects defined by averaging over 15 min runs for each of which (again) $S_0 \geq 1.5$ m s^{-1} and the mean wind approached the main hedge at an oblique angle ($\phi_0 = 45 \pm 8°$), the northeast wind transect being an average over 11 runs, the northwest over 14 runs. As noted (e.g.) by Heisler and DeWalle, "for natural barriers, as (obliquity) increases, the effective porosity of the windbreak along the direction of the wind becomes smaller". However since the permeability of the present hedge is already low, the further decrease in permeability due to oblique flow could be expected to have small effect (e.g. computations by Wang and Takle, 1996) and roughly speaking, this is what Fig. 4 indicates.

It is apparent from Fig. 4 that for winds from the east or northeast, mean windspeed was not invariant further windward than about $5H$, as would have been expected upwind of a long, straight and isolated shelterbelt (at the risk of oversimplification, in order to focus on the effect of the main hedge we normalized the transect of the east wind not on the farthest available upwind anemometer, but on a nearer anemometer at $x/H = -8.5$). Most probably the gradient in windspeed upwind from the main hedge, seen in east and northeast flows, results from the entry of the flow into a space not only barred downwind by the main hedge, but inhibited also by the perpendicular barriers (C and D in Fig. 1), and perhaps the slight slope. For winds from the west or northwest, farther upwind than about $4H$ the windspeed *was* quite constant—though this was not necessarily to be expected, in view of the upslope approach from the west, and the potential influence of other trees (E, Fig. 1).

So much for the depth and location of the minimum in the wind reduction curve: what of the leeward recovery? Recall that the pattern of mean wind reduction behind a thin, porous shelter varies systematically with the obliquity and stratification of the flow: with an increasingly oblique (or thermally unstable) approach wind, the amplitude and span of the wind reduction curve are reduced, the point of minimum windspeed moving closer to the fence and the leeward recovery occurring more promptly[4] (e.g. Seginer, 1975). Fig. 5 compares mean windspeeds from the cups and sonics during a single thermally unstable

[4] This implies that one ought not to expect identical relative windspeed curves in a pair of periods sharing the same mean θ_0, but very different standard deviations σ_{θ_0}, of reference wind direction.

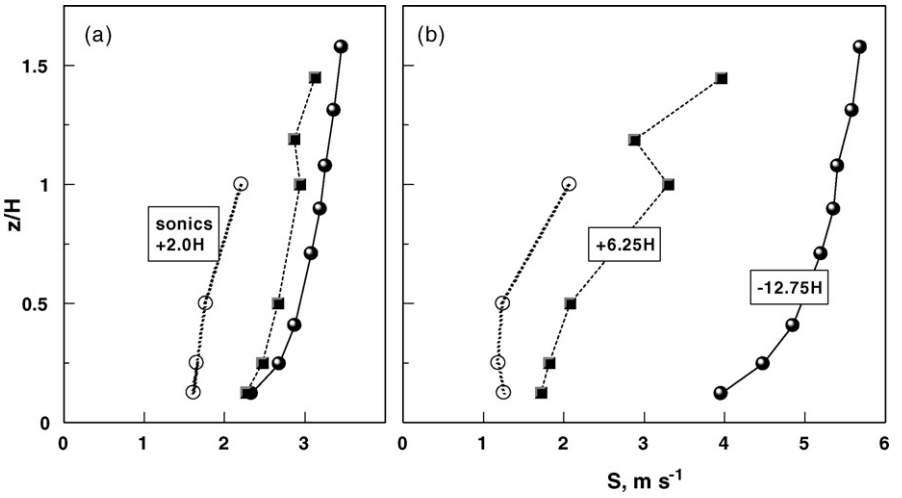

Fig. 6. Profiles of mean cup windspeed S upwind and downwind from the hedge, for oblique flows ((a) $\phi_0 = 52^\circ$; (b) $\phi_0 = 32^\circ$) in the NE quadrant (compass wind directions from the sonic on the east tower at $x/H = -12.75$, $\theta_0 = 38^\circ, 58^\circ$). The profiles at $x/H = (-12.75, +6.25)$ were provided by cup anemometers, and those at $x/H = +2$ by sonic anemometers.

30-min period ($L = -6$ m, $\phi_0 = 33^\circ, \theta_0 = 57^\circ, \sigma_{\theta_0} = 41^\circ$) against nine (15 min mean) re-scaled wind reduction curves from a much windier, overcast day ($37^\circ \leq \theta_0 \leq 53^\circ$; mean and standard deviation of the nine individual σ_{θ_0} were 25°, 4°; cup windspeeds at 2 m at $x/H = 12.75$ spanned $4.1 \leq S \leq 5.3$ m s^{-1}). Evidently the recovery in the lee of this low permeability hedge is much more prompt during periods of unstable stratification, than in near neutral flows, just as it would be behind a thin permeable windbreak. And Fig. 6, which compares lee-side vertical profiles of mean windspeed in highly oblique ($\phi_0 = 52^\circ$) and much less oblique ($\phi_0 = 32^\circ$) winds, confirms the anticipated effect of obliquity: in the highly oblique run, winds only 6H leeward of the hedge already have recovered to within about 90% of the approach value, whereas in the less oblique flow they stand at a much lower ∼50% of the reference.

Returning to the transects of Fig. 4, we can say that if the winds are not too oblique and stability is not too far from neutral, mean windspeed in the lee recovers in qualitatively the same fashion as behind a thin porous fence, i.e. over a distance of order 20H. However in the particular case of an approach flow from the east, the instruments reveal an anomaly at our site, in that beyond circa 4H downwind the recovery does not continue. This leeward ''plateau'' in mean windspeed may relate to the fact that the leeward flow is a downslope flow; for according to the analysis of slope flow by Jackson and Hunt (1975), in upslope (downslope) flow an induced pressure gradient is liable to enhance (curtail) the windspeed. However the only way to be sure would be to model this flow in its complexity (terrain; stratification, multiple belts), and so we mention this possibility only to emphasize the many factors in play, at this site.

3.2. Influence of secondary shelterbelts

We turn now to a more complex transect when the direction of the mean wind is such as to definitively implicate other windbreaks. Fig. 7 gives a single 30 min transect in mean windspeed for winds from the southeast (note the good conformity between mean windspeeds from the sonics and from the cups, already evidenced by Fig. 5). The most striking feature is a ''jet'' hard against the windward side of the windbreak,

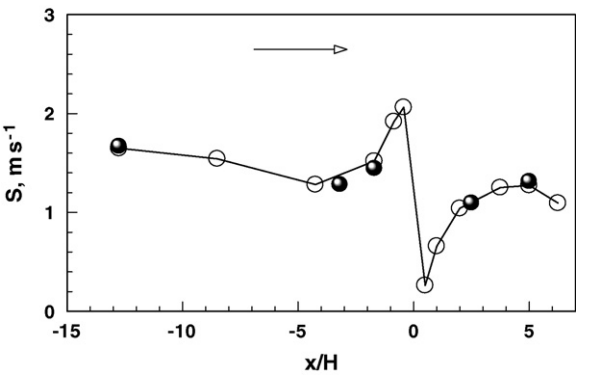

Fig. 7. Transect along $z = 2$ m of 30 min mean cup windspeed S, from sonics and from cups. The approach flow is from the SE (the sonic on the eastern tower measured $\theta_0 = 139^\circ$; a vane on the western tower measured $\theta = 159^\circ$). *Note*: the easternmost sonic stood at $z = 5$ m, thus (here) the speed it indicated has been reduced by the factor $\ln(2/z_{0E})/\ln(5/z_{0E}) = 0.87$.

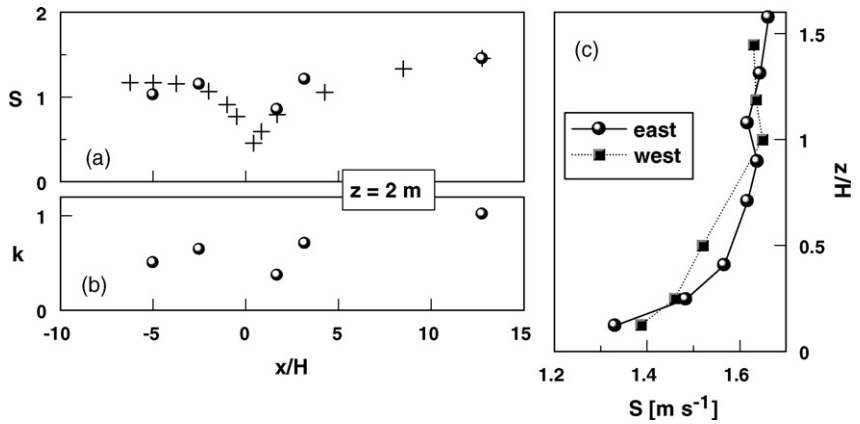

Fig. 8. Flow from the north, i.e. parallel to the main hedge. Panels (a) and (b) give transects of mean velocity S (m s^{-1}) and turbulent kinetic energy k (m^2 s^{-2}) (solid symbols are sonic measurements). Panel (c) gives the mean profiles of cup windspeed on the east and west towers. (*Note*: the TKE measurements from the reference sonic at $x/H = +12.75$ have *not* been adjusted to account for the differing (2 m) height of the other sonics on the transects.)

whereas on the leeward side one observes the same (high) degree of shelter $\Delta S/S_0 \sim 0.8$ as seen for east, west, northeast and northwest flows. Referring to Fig. 1, one notes that the fetch upwind from the main windbreak, for southeast flows, is interrupted by a perpendicular line of weeping willows (D) and that this line is terminated upwind of the main hedge (A) by an opening. The windward jet is almost certainly attributable to the gap, and it occurred without fail (and with constant signature) in southeasterly winds.

Fig. 8 covers a single 30 min run during a light, unstable, northerly flow *parallel* to the main hedge (from the reference sonic at 5 m on the east tower: $\theta_0 = 1^\circ$, $u_* = 0.29$ m s^{-1}, $L = -17$ m, $S = 1.57$ m s^{-1}, normalized turbulent kinetic energy $k/u_*^2 = 12.1$; a thin, high overcast was noted). In this case the main hedge (A in Fig. 1) should exert an influence only in its immediate vicinity (i.e. small $|x|/H$). However the instruments on the transect and towers lay roughly 200 m (order $25H$) downwind from another, northern shelterbelt (C in Fig. 1). Over most of its length the northern shelterbelt (C) was a dense, pruned hedge with a height of about 8 m, however along its westernmost 100 m or so it was constituted by taller (circa 20 m) individual trees. The relative windspeed curve Fig. 8a demonstrates approximate east–west reflection symmetry, despite the imperfect symmetry of shelterbelt C, the uneven distances of the anemometers from it, and the existence of the trees (B) that effectively widen the main hedge on its eastern side. From Fig. 8a the drag of the main hedge A (and trees, B) had an observable effect as far distant as about $3H$ from its faces. Fig. 8c confirms this east–west symmetry in that the mean wind profiles at either end of the transect were very similar. Fig. 8b gives the corresponding transect of turbulent kinetic energy (TKE, k) and indicates some reduction near hedge A, though the most striking point is that (curiously) the transects of S, k are similar—indeed for the four sonics measuring at $z = 2$ m, the dimensionless ratio k/S^2 lay in the narrow range $0.48 \leq k/S^2 \leq 0.51$ (it would be interesting to know the extent to which this finding generalizes, across complex sites like this).

3.3. Pattern of the turbulent kinetic energy in traversing winds

Profiles of turbulent kinetic energy in the near lee of the hedge at $|x|/H = 2$ (Fig. 9a) show the expected 'quiet zone' below $z/H = 1$. In highly oblique flow the quiet zone is shallower, i.e. (assuming one may interpolate along z/H) over much of the profile the TKE equals or exceeds the reference (upwind) value k_{ref} measured on the eastern mast. The transect Fig. 9b, performed in north-easterly, unstably-stratified winds, shows an unexpected gradient in TKE between locations distant $|x/H| = 1.7, 3.2$ upwind of the hedge, a feature of most of the transects for north-easterly flows, and which may reflect an influence of the northern hedge (C, Fig. 1) and/or the trees (B). In any case it appears that the region of protection afforded by the main hedge, in terms of reduced turbulence (say, $k/k_{\mathrm{ref}} < 50\%$) is narrow.

3.4. Velocity at the two sides of the hedge: wind 'refraction'

A hedge filters the penetrating airstream, and so the entry and exit winds are pertinent to the theory of aerosol deposition (e.g. Raupach et al., 2001; Wilson,

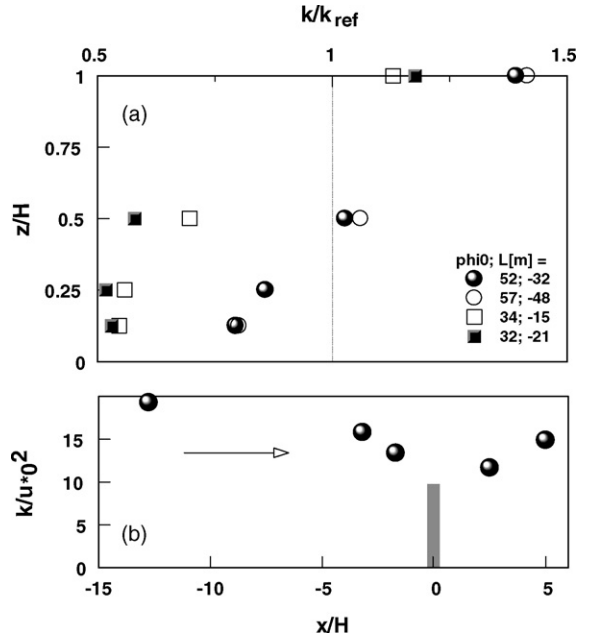

Fig. 9. Normalised turbulent kinetic energy in periods of NE winds (30 min averages). Panel (a), vertical profile of k/k_{ref} in the near wake at $|x/H| = 2$, as function of the orientation of the flow (ϕ_0 expressed relative to the normal to the hedge); Panel (b), a single 30 min transect k/u_{*0}^2 ($\phi_0 = 47^\circ$, $u_* = 0.26$ m s^{-1}, $L = -16$ m). Normalizing scales k_{ref}, u_{*0}^2 from the sonic at $z = 5$ m on the east tower.

2005; Bouvet et al., 2007). Therefore it seemed interesting to compare velocity statistics on the entry and exit faces, and to this end as one of the three experimental configurations we placed the two CSAT3 sonic anemometers, still at height $z = 2$ m ($z/H = 1/4$) and sampling at 5 Hz,[5] against the sides of the main hedge. Figs. 10 and 11 give 20-min time series (27 August 1100–1120 UTC) of the normal (u) and parallel (v) velocity components on the two faces (1, 2: upwind, downwind) of the hedge, these traces resulting from application of a rectangular moving-average filter (101 samples, for a window width of ± 20 s) to the raw series.[6] When the normal component is from the east (i.e. $u_{\mathrm{E}} > 0$, where the attached subscript E or W will signify the measurement has been made on the east or west face), it has the same sign but a smaller magnitude on the western (i.e. leeward) face of the hedge, i.e. $u_{\mathrm{E}} > u_{\mathrm{W}} > 0$. Conversely, if the normal component is from the west (wind from the western quadrants), $u_{\mathrm{W}} < u_{\mathrm{E}} < 0$. This is as expected. But what is more striking is that the parallel component of the wind (v) is very small on the leeward side of the hedge. This effect (i.e. an observed 'refraction' of the mean wind vector towards the normal) had been previously reported by Nord (1991; her Fig. 13) for the case of a dense shelterbelt composed of multiple rows of trees, and also was suggested by the computations of Wang and Takle (1995).

Tables 1 and 2 give entry and exit wind statistics computed directly from the unfiltered time series, for periods excluding wind reversal. During the period $1 \leq t \leq 6$ min of the record of Figs. 3 and 4, a period (Run 5 of Tables 1 and 2) when the wind blew from the northeast (compass direction $\theta_1 = 36^\circ$) to impinge on the eastern side of the hedge at an angle $\phi_1 = 54^\circ$ ($=90^\circ - 36^\circ$) relative to the normal, mean wind direction ($\theta_2 = 90^\circ$) at the exit to the hedge was oriented down the normal.[7] During $9 \leq t \leq 16$ min (Run 6), northwesterly winds ($\theta_1 = 343^\circ$) impinged on the western side of the hedge, and again the exiting wind blew down the normal ($\theta_2 \approx 270^\circ$). This pattern was confirmed in every such period available for analysis. We conclude that a long, tall, thick hedge strongly absorbs the transverse momentum flux ($UV + \overline{u'v'}$) such that at the leeward edge the mean parallel velocity component essentially vanishes, and the fluctuating parallel component is small. This is somewhat analogous with the rapid attenuation by a dense uniform plant canopy (height H) of the entrant vertical momentum flux $\overline{u'w'}$, an attenuation which results in roughly an exponential decay of the mean velocity $U(z)$ as one descends into the canopy, with low levels of mean and turbulent velocity on ground. And it contrasts with the case of a thin, porous planar barrier (e.g. lattice fence), where the swing of the wind towards the normal is incomplete and the discontinuity in wind direction across the barrier can be related (Taylor and Batchelor, 1949) to the resistance coefficient k_{r} of the barrier.

But why is the parallel component (v) almost completely attenuated by the hedge, while the normal component (u), although markedly reduced, does penetrate? Recall that the windward normal (entrant) velocity $u_1 = u(-X/2, z)$ entails a mass flux $\rho u_1(z)$ into the volume of the hedge, while the parallel component

[5] We did not apply any coordinate rotation to the sonic signals, which would have been inappropriate in this disturbed flow.

[6] Different sampling rates and inexactly synchronized clocks disallowed direct comparison with a second sonic anemometer at $z = 2$ m at the eastern side of the hedge. However the signal from this Gill sensor several metres distant from the CSAT3 (see Fig. 2) showed qualitatively the same behaviour as the latter.

[7] An exact coincidence of the computed exit wind direction with the nominal orientation of the normal to the hedge, i.e. 90° or 270°, could only be fortuitous: the sonic anemometers had been aligned in azimuth relative to the hedge by eye alone.

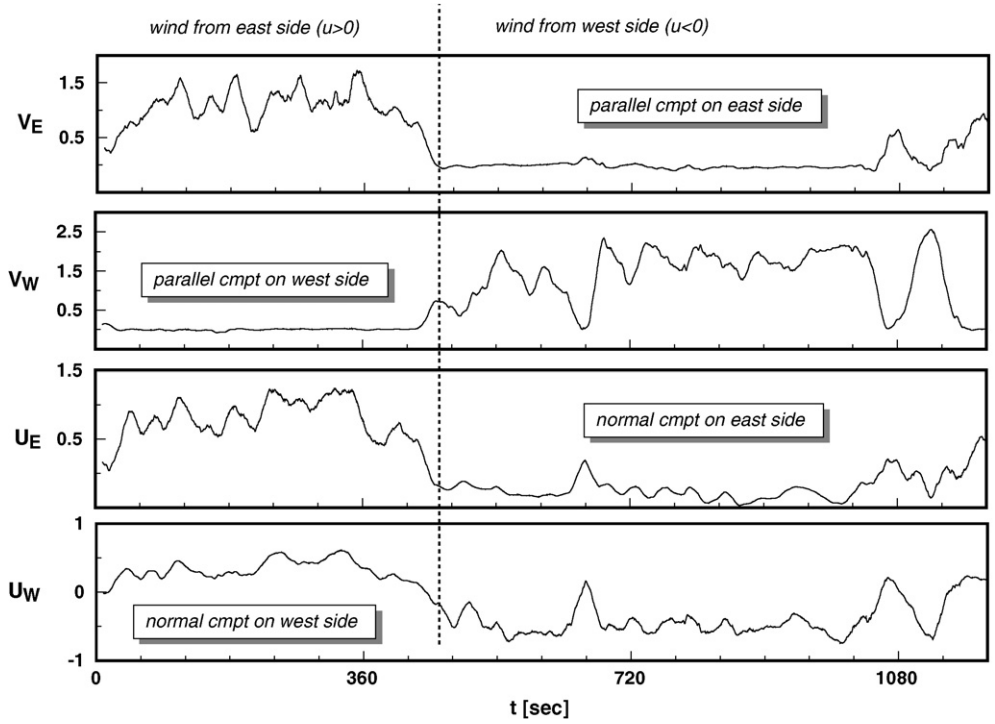

Fig. 10. Twenty minute record of the lowpass filtered horizontal velocity components (m s^{-1}), measured at $z = 2$ m hard against the east and west sides of the hedge. During the interval $1 \leq t \leq 7$ min, wind was from the eastern quadrants, and during $9 \leq t \leq 17$ min predominantly from the western quadrants.

does not (ρ is air density). By conservation of mass, we know that the total entrant air mass flux is balanced by the sum of the (appropriate area integrals of) leeward exit flux $\rho u_2(z)$ and the hedge-top exit flux $\rho w(x, H)$. To a first approximation, the dominant exit flux will be down the path of least resistance, and so (for the case of a uniform foliage area density, anyway) related to the ratio X/H of the width to the height of the hedge. By that

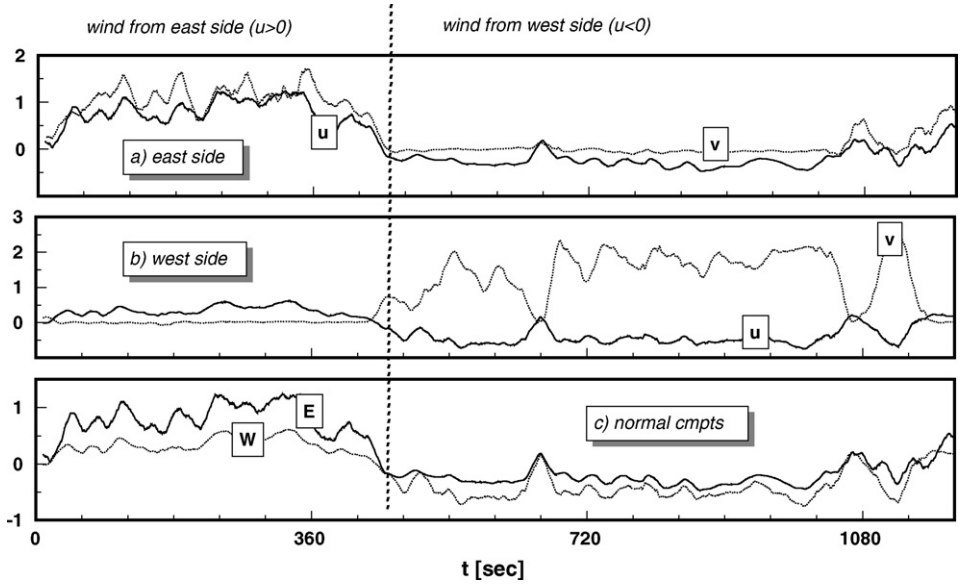

Fig. 11. Same as Fig. 10, but with signals paired to show (a and b) the two components on each face, and (c) attenuation of the normal component u, and showing the switch in its sign and relative magnitude on east and west sides as wind direction switches from easterly to westerly.

Table 1
Mean wind directions (θ) at entry and exit faces of the hedge (aligned north–south), for several periods selected by the criterion that mean wind direction did not traverse 180° or 360°

Run	Date	Interval	Meteo	S_1	Side	$\tan^{-1}(V/U)$	$\overline{\tan^{-1}(v/u)}$
1	23 Aug	1704–15	Frwthr Cu hot; vrble wnd	0.76	E*	152°	192°
					W	85°	83°
2	24 Aug	1115–26	Clear; vrbl wnd	0.58	W*	231°	173°
					E	276°	276°
3	24 Aug	1238–00	Clear; vrbl wnd	1.21	E*	154°	210°
					W	91°	89°
4	24 Aug	1332–44	Clear; vrbl wnd	0.83	W*	295°	73°
					E	265°	262°
5	27 Aug	1101–06	Hvy ovrcst	1.48	E*	36°	34°
					W	90°	89°
6	27 Aug	1109–16	Hvy ovrcst	1.71	W*	343°	346°
					E	266°	269°
7	27 Aug	1138–47	Hvy ovrcst	0.83	E*	23°	13°
					W	89°	82°

The star (e.g. E*) identifies the upwind face, and S_1 (m s^{-1}) is the cup windspeed measured by the sonic on the upwind face, i.e. $S_1 = \overline{\sqrt{u_1^2 + v_1^2}}$. For a mean wind normally incident (alt. exiting) on the east side $\theta = 90°$ (alt. 270°), while for a mean wind normally incident on the west side $\theta = 270°$. *Note*: where a velocity component undergoes major fluctuations the calculation $\overline{\tan^{-1}(v/u)}$, which could be called "the mean angle of the wind vane", may be problematic due to the periodic discontinuity of the circular functions.

reasoning a hedge with small X/H will probably have a distinct leeward exit current (u_2) and relatively weak $w(H)$, and vice versa.

3.5. Drag parameter diagnosed from the relative wind-speed curve and from hedge-face wind statistics

There has been much discussion of what is an easily measured characteristic of a natural windbreak that adequately indexes the shelter it provides in its lee (Heisler and DeWalle, 1988; Nelmes et al., 2001). Zhou et al. (2004) recommend the use of a detailed structural description, rather than superficial optical parameters (e.g. porosity) or aerodynamic parameters such as the depth $\Delta S/S_0$ of the relative windspeed curve at the point $(x = \breve{x})$ of lowest mean windspeed, or similar but more complex indices such as (Nelmes et al., 2001)

$$s = \sqrt{\frac{(U^2 + \sigma_u^2)_{(-H)}}{(U^2 + \sigma_u^2)_{(+H)}}}.$$

We did not make detailed structural measurements of the hedge and nor did we happen to have placed sonic anemometers so as to be able to determine "s". However we can assign an aerodynamic index (drag parameter) for the hedge as follows.

From the cup anemometer transects along $z = 2$ m during normally incident winds, we inferred earlier that at the most sheltered point $(\breve{x})$ the fractional reduction in mean cup windspeed was $\Delta S/S_0 \approx 0.75$ (where S_0 is the mean cup windspeed far upwind). Wilson et al. (1990) gave a correlation[8]

$$\frac{\Delta S}{S_0} = \frac{k_r}{(1 + 2k_r)^{0.8}} \quad (1)$$

Table 2
Ratios of wind statistics on the upwind (1) and downwind (2) sides of the hedge

Run	S_2/S_1	$\bar{u}_2/\bar{u}_1$	$\bar{v}_2/\bar{v}_1$	σ_{u2}/σ_{u1}	σ_{v2}/σ_{v1}	γ
1	0.26	0.58	0.027	0.51	0.14	3.2
2	0.47	0.78	0.11	0.46	0.088	No fit!
3	0.21	0.55	−0.0043	0.44	0.095	3.0
4	0.36	0.78	0.14	0.47	0.054	No fit!
5	0.25	0.42	−0.0011	0.40	0.10	2.7
6	0.18	0.58	0.014	0.54	0.11	3.0
7	0.27	0.59	−0.0027	0.52	0.19	3.0

The value given for γ is that which, if applied in Eq. (6), reproduces $c_d a = 1.8$ m^{-1}.

[8] This correlation originates from the numerical study by Wilson (1985), which focused on the field experiment of Bradley and Mulhearn (1983). However the formula is in no way 'calibrated', and subsequent work (e.g. Taylor, 1988; Wilson, 2004) supports its generality.

between the fractional wind reduction seen at the point of lowest mean wind-speed ($x = \breve{x}$) behind a simple porous fence, and the resistance coefficient k_r of that barrier. Strictly, this formula does not apply to a thick natural windbreak. If, however, we take it to imply the value of an effiective resistance coefficient, we may relate the latter to aerodynamic properties of the hedge thus:

$$k_r^{\text{eff}} = \int_{-X/2}^{X/2} c_d a \, dx = \overline{c_d a}\, X \tag{2}$$

Here we have used the mean value theorem, and $\overline{c_d a}$ is the mean value of the product of the bulk drag coefficient c_d and the drag area density presented by the vegetation. With $\Delta S/S_0 \approx 0.75$ it follows that $k_r^{\text{eff}} \approx 5.5$ and $\overline{c_d a} \approx 1.8\,\text{m}^{-1}$.

It is of interest to know whether this aerodynamic parameter of the hedge might be derivable from the sonic measurements on the two faces. Assuming a steady state prevails, the U-momentum equation is

$$\frac{\partial}{\partial x}(U + \overline{u'^2} + P) + \frac{\partial}{\partial z}(UW + \overline{u'w'}) = -c_d a U\sqrt{U^2 + V^2} \tag{3}$$

where P is the kinematic pressure disturbance, and the sink on the r.h.s. parameterizes drag on the vegetation. Upon integrating across the windbreak along the line joining the two anemometers, it *may* be reasonable to drop the term involving $UW + \overline{u'w'}$, in which case

$$[U^2 + \overline{u'^2} + P]_{+X/2}^{-X/2} \approx c_d a \int_{-X/2}^{+X/2} U\sqrt{U^2 + V^2}\, dx \tag{4}$$

Hypothesizing that

$$\Delta P = [P]_{+X/2}^{-X/2} = \gamma[U_1\sqrt{U_1^2 + V_1^2} - U_2^2] \tag{5}$$

where γ is an unknown constant (that should depend only weakly on measurement height), the l.h.s. of Eq. (4) can be estimated from the sonic signals on the upwind (''1'', $x = -X/2$) and downwind (''2'', $x = +X/2$) faces. Taking the simplest (i.e. linear) variation[9] of $U\sqrt{U^2 + V^2}$ across the windbreak in order to determine the coefficient of $c_d a$ in Eq. (4), we have

$$c_d a = \frac{(U_1^2 - U_2^2) + (\sigma_{u1}^2 - \sigma_{u2}^2) + \gamma(U_1\sqrt{U_1^2 + V_1^2} - U_2^2)}{X(U_1\sqrt{U_1^2 + V_1^2} + U_2^2)/2} \tag{6}$$

[9] Other simple choices proved less satisfactory.

Table 2 lists which value of γ, treated as a parameter free to be adjusted for any particular averaging interval over which wind direction did not reverse, ensures that Eq. (6) produces the value $c_d a = 1.8$. A value fixed at $\gamma = 3$ yields a value of $c_d a$ that is within an acceptably narrow range about the wanted (that is, the observed) value, lending some credibility to Eq. (6). On two occasions for which U_2/U_1 was larger, a far greater value of γ is called for.

We did wonder whether information on the density and drag of the hedge might be retrievable from lagged cross-covariances $\overline{u_1'(t)u_2'(t+\zeta)}$ between the normal velocity fluctuations on the two sides, on the principle that the response at the leeward face (2) to arrival of a gust at the entrant face (1) might be delayed (ζ the time lag) by drag on the vegetation: if so, the time lag ζ^* yielding *maximum* covariance might be a function of aerodynamic properties, e.g. $\zeta^* U_1/X = F(c_d, aX, \ldots)$. However computed maximum correlations lay at $\zeta = 0$ in all but two of the seven cases of Table 2, while in the other cases (6, 7) peaks were so wide that the lag value (ζ^*) at which the covariance was maximal was not sharply defined. Those two cases did tentatively confirm an expected relationship $\zeta^* \propto |U_1|^{-1}$ (lag between upwind and downwind fluctuation inversely proportional to normal component of entry velocity), though actually there was a tighter accord between the two values of $\zeta^* S_1$ (where S_1 is the entry speed), viz. $\zeta^* S_1 \approx 1.5$ s.

4. Conclusion

At this site we expected the pattern of the mean winds and turbulence would be complex, in response to interactive influences of the main hedge, other shelterbelts and trees, gateways and (perhaps) the gentle terrain slopes. However the transects and profiles we have identified do not differ at a *qualitative* level from what one might have anticipated on the basis of previous studies of dense windbreaks in the literature, confirming (once again) that micro-meteorological concepts drawn from studies of ideally symmetric flatland scenarios may give a useful first approximation for less ideal regimes.

During this experiment winds were generally light, and not uncommonly during a given 90 min time series wind direction changed sufficiently so as to exchange (several or many times) the designation 'upwind/downwind'. It would have been impossible to apprehend the interesting connection between the statistics of entry and exit winds without filtering in regard to these 'exchanges' of the upwind/downwind role: conditional

sampling is essential if one is to obtain intelligible wind statistics, in a complex flow of this type.

Acknowledgements

We thank Olivier Zurfluh (INRA) for assistance in the field, and Monsieur Verkest of the Villepreux farm for hosting the experiment. Financial support has been provided by INRA, by the Natural Sciences and Engineering Research Council of Canada (NSERC), and the Canadian Foundation for Climate and Atmospheric Studies (CFCAS). Two anonymous reviewers provided numerous helpful suggestions for the improvement of this manuscript, and we are most grateful to them.

References

Agate, E., 2002. Hedging. A Practical Handbook. BTCV Handbook. BTCV, ISBN: 0946752176, 125 pp.

Bouvet, T., Loubet, B., Wilson, J.D., Tuzet, A., 2007. Filtering of windborne particles by a natural windbreak''. Boundary-Layer Meteorol. 123, 481–509.

Bradley, E.F., Mulhearn, P.J., 1983. Development of velocity and shear stress distributions in the wake of a porous shelter fence. J. Wind Eng. Indust. Aerodyn. 15, 145–156.

Caroupanapoullé, C., 2004. Analyse et modélisation de l'effet d'une haie sur le bilan radiatif d'une parcelle dans le domaine solaire. Mémoire de thèse, INA-PG, Université Paris 6, ENS, UMR INRA INAPG Environnement et Grandes Cultures de Grignon, 154 pp.

Heisler, G.M., DeWalle, D.R., 1988. Effects of windbreak structure on wind flow. Agric. Ecosys. Environ. 22/23, 41–69.

Jackson, P.S., Hunt, J.C.R., 1975. Turbulent wind flow over a low hill. Quart. J. R. Meteorol. Soc. 101, 929–955.

Nelmes, S., Belcher, R.E., Wood, C.J., 2001. A method for the routine characterisation of shelterbelts. Agric. Forest Meteorol. 106, 303–315.

Nord, M., 1991. Shelter effects of vegetation belts—results of field measurements. Boundary-Layer Meteorol. 54, 363–385.

Plate, E.J., 1971. The aerodynamics of shelter belts. Agric. Meteorol. 8, 203–222.

Raupach, M.R., Woods, N., Dorr, G., Leys, J.F., Cleugh, H.A., 2001. The entrapment of particles by windbreaks. Atmos. Environ. 35, 3373–3383.

Rider, N.E., 1952. The effect of a hedge on the flow of air. Quart. J. Royal Meteorol. Soc. 78, 97–103.

Seginer, I., 1975. Flow around a windbreak in oblique wind. Boundary-Layer Meteorol. 9, 133–141.

Takahashi, H., 1978. Wind tunnel tests on the effect of width of windbreaks on the wind speed distribution in leeward. J. Agric. Met. 33 (4), 183–187.

Taylor, P.A., 1988. Turbulent wakes in the atmospheric boundary layer. In: Steffen, W.L., Denmead, O.T. (Eds.), Flow and Transport in the Natural Environment: Advances and Applications. Springer-Verlag, pp. 270–292.

Taylor, G.I., Batchelor, G.K., 1949. The effect of wire gauze on small disturbances in a uniform stream. Quart. J. Mech. Appl. Math. 2, 1–29.

van Eimern, J., Karschon, R., Razumova, L.A., Robertson, G.W., 1964. Windbreaks and Shelterbelts. World Meteorol. Org., Tech. Note No. 59.

Wang, H., Takle, E.S., 1995. Numerical simulations of shelterbelt effects on wind direction. J. Appl. Meteorol. 34, 2206–2219.

Wang, H., Takle, E.S., 1996. On shelter efficiency of shelterbelts in oblique winds. Agric. For. Meteorol. 81, 95–117.

Wilson, J.D., 1985. Numerical studies of flow through a windbreak. J. Wind Eng. Indust. Aero. 21, 119–154.

Wilson, J.D., 2004. Oblique, stratified winds about a shelter fence. I. Measurements. J. Appl. Meteorol. 43, 1149–1167.

Wilson, J.D., 2005. Deposition of particles to a thin windbreak: the effect of a gap. Atmos. Environ. 39, 5525–5531.

Wilson, J.D., Swaters, G.E., Ustina, F., 1990. A perturbation analysis of turbulent flow through a porous barrier. Quart. J. R. Meteorol. Soc. 116, 989–1004.

Zhou, X.H., Brandle, J.R., Mize, C.W., Takle, E.S., 2004. Three-dimensional aerodynamic structure of a tree shelterbelt: definition, characterization and working models. Agrofor. Syst. 63, 133–147.